

IMPROVED MODELING OF SHARP ZONES IN RESONANT PROBLEMS

WITH THE TLM METHOD

J.A. Morente, J.A. Portí, H. Magán, and O. Torres

Department of Applied Physics. Faculty of Sciences. University of Granada
18071, Granada (Spain). Telephone 34-58-243229. Telefax 34-58-243214
e-mail address: jporti@goliat.ugr.es

ABSTRACT: Several new modified nodes based on the symmetrical condensed node with stubs are proposed to solve the difficulty of the TLM method in modeling problems highly dependent on frequency. These nodes avoid the problem of indirect modeling at critical points, such as bends and corners, thus providing more accurate results and flexibility in the modeling of conducting parts. The new nodes are applied to specific problems of rectangular waveguides loaded with rectangular irises of finite width to verify their capability to predict resonant phenomena.

1 INTRODUCTION

Time-domain numerical methods are a powerful and useful tool for solving electromagnetic and other physical broadband problems. These methods allow nearly direct treatment of non-linearities, non-homogeneities, time-varying systems, and other situations. However, the most outstanding characteristic of time-domain algorithms is that they provide information for a wide range of frequencies in only one time-domain computer run. Results obtained by these methods have proven to be satisfactory for many practical applications; nevertheless, in specially difficult situations such as resonant problems, large memory and CPU time are often required.

The difficulty of accurately predicting resonances with the Transmission Line Modeling method (TLM method) is not new and has been discussed in the literature for certain specific cases [1]- [3]. In [1] the origin of the problem is explained by the difference between the path length followed by the individual voltage pulses at the TLM nodes near sharp zones and the actual path they should follow in the original problem. The difference in length turns into a delay or advance in time and thus into a shift in frequency. This frequency displacement is also related to the rapid variation of the field distribution at these points, behavior that a coarse mesh is unable to reproduce [4]. A very fine mesh would solve these problems, but would be extremely expensive in memory and CPU time requirements. The problem is solved in [1] by modifying the properties of the medium close to a wire in order to adapt the speed of the pulses that surround the wire and so eliminate the time delay appearing in the standard TLM solution.

Despite the satisfactory results provided by this solution, it presents the disadvantage of requiring the modification of

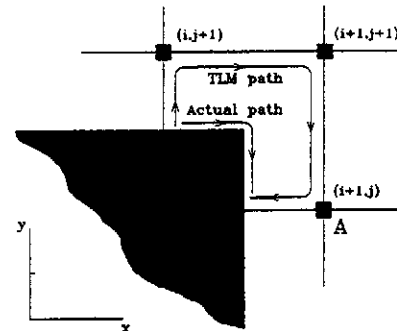


Fig.1.- Indirect modeling of a 2D corner

the surrounding medium instead of dealing with the actual problem, the indirect modeling of sharp regions. The standard modeling of conducting zones short-circuits the link lines between nodes, however the information of the conducting geometry is available from not only one node but from a set of adjacent nodes. The situation is shown in Fig. 1 for a bidimensional conducting corner located at the (i,j) node. The corner is modeled by short-circuiting link lines between nodes (i,j) and $(i+1,j)$, and link-lines between nodes (i,j) and $(i,j+1)$, letting voltage pulses travel freely from these nodes to node $(i+1,j+1)$. This means that the information fully describing the corner is contained in four adjacent nodes, two nodes in each cartesian direction. The corner is in practice modeled by a coarser mesh two-nodes wide and it may therefore represent an important source of numerical errors. One way to lessen these errors is to develop new nodes that directly model complex geometries without the need of using adjacent nodes. This idea was applied in [2] for treating half conducting planes by including modifications to the standard symmetrical condensed node without stubs, that is to say, using the same mesh size in each cartesian direction. Finally, a specific treatment of edges and corners with the TLM method has recently been presented in [3] for the modified version of the method known as the Alternating Transmission Line Matrix scheme.

Many practical situations must take into account numerous complex geometries in addition to that presented in [2]. Moreover, it would be useful if the modified nodes allowed the use of a different mesh size in each cartesian direction, and therefore the inclusion of inductive and capacitive stubs

is advisable. The aim of this paper is the numerical modeling of resonant problems, such as microwaves loaded with rectangular irises of finite width. As will be shown, the standard TLM treatment of these problems reveals a significant shift in the resonant frequencies, so a number of new TLM nodes with stubs providing accurate but low-cost solutions will be presented and tested for both resonant and non-resonant situations.

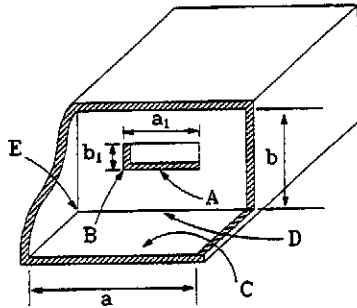


Fig.2.- Geometry of the problem

2 SPECIAL NODES

A typical geometry of a resonant problem is a waveguide loaded with a rectangular iris of finite width (Fig.2). Let us propose some new TLM nodes with stubs that represent a direct model of the specific region and also allow the numerical field to follow the path of the actual field. A great number of nodes can be developed, but only those necessary for the modeling of the problem sketched in Fig.2 will be presented in this paper.

The first node presented is the transmission-line model of a 90° bend in a conducting object oriented as shown in Fig.3, corresponding to point A in Fig.2. The node is a symmetrical condensed node with stubs (not represented) including several modifications. First, those standard-node lines that are completely short-circuited by the conducting planes have been removed. Second, those lines that are partially short-circuited now have a characteristic impedance or admittance proportional to the part that has not been short-circuited. By doing so, for example, lines 1 and 13, associated with E_x , have been removed, the characteristic impedance of lines 3 and 5 is $Z_0/2$ and Z_0 , respectively, $Z_0=1/Y_0$ being the characteristic impedance of the standard-node link-lines. Finally, the capacitive stub in the y-direction, line 14, has an admittance of $7Y_y Y_0/4$, Y_y being the relative admittance of the line in the original node with stubs. This value is obtained by considering that the capacitive stub E_y of original admittance $Y_y Y_0$, is formed of four capacitive lines of admittance $Y_y Y_0/4$, three of which are half short-circuited by the conducting planes.

The following preliminary form of the scattering matrix for this node can be obtained in the usual way by applying Maxwell's equations [5]:

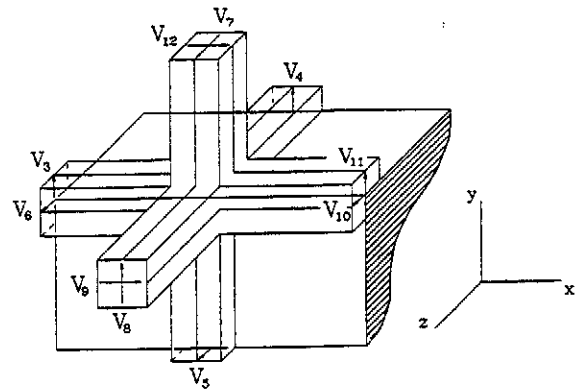


Fig.3.- Node for the 90° bend A in Fig. 2

	3	4	5	6	7	8	9	10	11	12	14	15	16	17	18
3	c	j				p			e	-b	ω				$-\lambda$
4	f	g	k		-o	n			f	ω		δ			
5		k	g	f	n	-o		f			ω	$-\delta$			
6			j	c	p		-b	e			ω		λ		
7		-h	i	f	l	m		f			ω	θ			
8	f	i	-h		m	l			f	ω		$-\theta$			
9				-d			a	d						σ	
10			j	e	p		b	c			ω	$-\lambda$			
11	e	j				p			c	b	ω				λ
12	-d								d	a					$-\sigma$
14	α	γ				ϵ			α	Ω					
15			γ	α	ϵ			α			Ω				
16		η	$-\eta$		ξ	$-\xi$							χ		
17				β			τ	$-\beta$						Δ	
18	$-\beta$								β	$-\tau$					Δ

(1)

where the different parameters are given by

$$a = \frac{Z}{4 + Z}, \quad b = \lambda = \frac{2}{4 + Z}, \quad k = o = \delta = \frac{d}{3},$$

$$c = \frac{Z}{2(4 + Z)} + \frac{4 - 7Y}{14(4 + Y)}, \quad d = \sigma = 2b,$$

$$e = -\frac{Z}{2(4 + Z)} + \frac{4 - 7Y}{14(4 + Y)}, \quad h = m = \theta = \frac{4}{3}b,$$

$$f = \alpha = \frac{16}{7(4 + Y)}, \quad g = \frac{Z}{3(4 + Z)} - \frac{8 + 14Y}{21(4 + Y)},$$

$$i = -\frac{2Z}{3(4 + Z)} - \frac{8 + 14Y}{21(4 + Y)}, \quad j = \gamma = \frac{16}{28 + 7Y},$$

$$l = \frac{2Z}{3(4 + Z)} - \frac{4 + 7Y}{21(4 + Y)}, \quad \beta = \tau = \eta = \xi = 2a,$$

$$n = -\frac{Z}{3(4 + Z)} - \frac{4 + 7Y}{21(4 + Y)}, \quad p = \epsilon = \frac{f}{2},$$

$$\omega = \frac{2Y}{4+Y}, \quad \Omega = \frac{Y-4}{Y+4}, \quad \chi = \Delta = \frac{4-Z}{4+Z}. \quad (2)$$

It must be noted that Y and Z in each parameter of (2) take the appropriate subscript according to the lines corresponding to it.

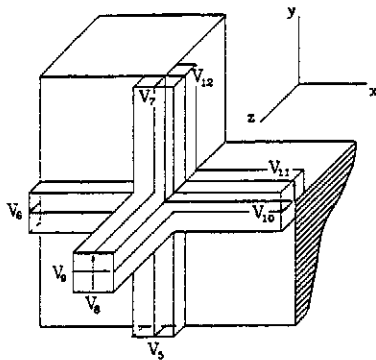


Fig.4.- Node for modelling point B in Fig.2

The second node that we propose for modeling a rectangular iris is shown in Fig.4. This node describes point B in Fig.2. The admittance or impedance of each line is obtained as for the preceding node. The scattering matrix for this node is:

	5	6	7	8	9	10	11	12	15	16	17	18
5	a	c	b	-h		c				n	-p	
6	c	a	c		-h	b				n		p
7	b	c	a	h		c				n	p	
8	-d		d	g								-q
9		-d			g	d						q
10	c	b	c		h	a				n	-p	
11							j	k				s
12							k	j				-s
15	e	e	e			e				m		
16	-f		f	-i								o
17		f			i	-f						o
18							l	-l				r

(3)

where the parameters appearing in (3) are given by:

$$a = \frac{-Y}{2(4+Y)} + \frac{Z}{2(4+Z)}, \quad c = e = \frac{2}{4+Y},$$

$$b = \frac{-Y}{2(4+Y)} + \frac{-Z}{2(4+Z)}, \quad d = k = q = s = \frac{4}{4+Z},$$

$$f = i = l = \frac{2Z}{4+Z}, \quad g = j = \frac{f}{2}, \quad h = p = \frac{d}{2},$$

$$m = \frac{Y-4}{Y+4}, \quad n = \frac{2Y}{4+Y}, \quad o = r = \frac{4-Z}{4+Z}. \quad (4)$$

The flat conducting zones such as point C in Fig.2 are simulated with a half node similar to that presented in [2] but with three extra stubs to add the capacitance and inductance needed for synchronism. The modified scattering matrix for a flat conducting plate in the x-z plane is:

	3	4	7	8	11	12	14	16	18
3	a	c		c	b	-h	k		-n
4	c	a	-h	b	c		k		n
7			-d	g	d				m
8	c	b	h	a	c		k		-n
11	b	c		c	a	h	k		n
12	-d				d	g			-m
14	e	e		e	e		j		
16		f	i	-f					l
18	-f				f	-i			l

(5)

with the parameters given by:

$$a = \frac{-Y}{2(4+Y)} + \frac{Z}{2(4+Z)}, \quad c = e = \frac{2}{4+Y},$$

$$b = \frac{-Y}{2(4+Y)} + \frac{-Z}{2(4+Z)}, \quad d = m = \frac{4}{4+Z},$$

$$f = i = \frac{2Z}{4+Z}, \quad g = \frac{f}{2}, \quad h = n = \frac{d}{2},$$

$$j = \frac{Y-4}{Y+4}, \quad k = cY, \quad l = \frac{4-Z}{4+Z}. \quad (6)$$

In the case of the inner bends, such as point D in Fig.2, the planes short-circuit all the lines except three: link-lines 7 and 8, of characteristic impedance $Z_0/2$, and line 16 of characteristic impedance $Z_x Z_0/4$, Z_0 and Z_x being the corresponding values for the standard node. The scattering matrix is:

	7	8	16
7	a	b	e
8	b	a	-e
16	c	-c	d

(7)

where the parameters in (7) are given by:

$$a = \frac{c}{2} = \frac{Z}{4+Z}, \quad b = e = \frac{4a}{Z}, \quad d = \frac{4-Z}{4+Z}. \quad (8)$$

Finally, internal corners (point E in Fig.2) short-circuit all the lines in a symmetrical condensed node and, therefore, no scattering matrix is required at these points. This is a direct consequence of the field vanishing at this point. In fact, bend nodes adjacent to a particular corner have no lines directed to the corner, so there is no actual need for a corner node.

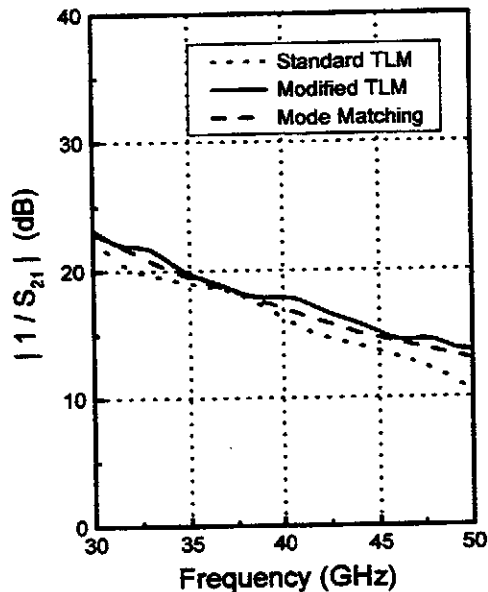


Fig.5.- Circuit S_{21} parameter for a WR28 waveguide with a non-resonant iris. Dimensions: $a=28$, $b=14$, $a_1=b_1=8$, and $t=2$, in Δl units where $\Delta l=0.25\text{mm}$.

3 NUMERICAL RESULTS

In order to establish the performances of the new nodes mentioned in the previous section, some circuit-S parameters of rectangular waveguides loaded rectangular irises have been calculated using the TLM method for both the standard mesh of symmetrical condensed nodes and for a mesh including the new nodes proposed above.

The first case studied is a WR28 rectangular waveguide of dimensions $a=2b=7.112\text{mm}$ with a non-resonant square iris with sides $a_1=b_1=2\text{mm}$ and a thickness of $t=0.5\text{mm}$. The mesh size, Δl in all the cartesian directions, is adjusted to exactly model the iris dimensions. Concretely, Δl is 0.25mm , so $a_1=b_1=8$, and $t=2$, in Δl units. With this node size, the waveguide transverse dimensions are $a=28$ and $b=14$ nodes length. These dimensions are of course identical for both TLM simulations, the only difference is that in the standard formulation conducting zones are halfway between

nodes, while in the modified scheme the whole geometry is displaced a distance $\Delta l/2$ in each Cartesian direction but the relative positions and sizes are maintained. In this manner any difference between both TLM simulations will be only due to the effect of the specific nodes. The time step used is $4.169 \cdot 10^{-13}$ s, which corresponds to the maximum allowable value for this mesh size. The waveguide has been excited by a Gaussian pulse with a bandwidth of 10GHz , modulated at 40GHz . To eliminate artificial reflections at the limit of the mesh, wide band absorbing conditions based on finite impulse-response filters theory have been used at both ends of the waveguide [6]. The amplitude of the S_{21} parameter for the standard and the proposed TLM solution is plotted in Fig.5, together with the TE_{10} mode matching results taken from [7] for comparison. Good behavior can be observed for the standard and the proposed solution. Nevertheless, although errors are of course present, there is no significant improvement since the problem is not critically dependent on the frequency such as a resonant problem would be. These similar results are also observed for the corresponding phase values. It is worth noting that this behavior can also be observed in open problems such as scattering ones. In fact, the standard and the proposed solution with different mesh size in each direction have been used for predicting the near field scattered by an infinitely long square conducting cylinder and by a conducting cube. As indicated above, results obtained show no significant differences between the amplitude and phase of both solutions.

The aim of the second example is to determine whether the similarity in behavior for the standard and the proposed TLM model still holds when applied to a problem that is critically dependent on frequency. The above-mentioned

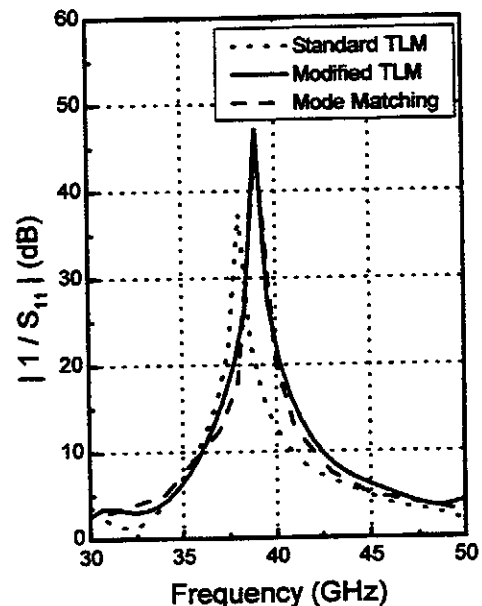


Fig.6.- Circuit S_{11} parameter for a WR28 waveguide with a resonant iris. Dimensions: $a=28$, $b=14$, $a_1=16$, $b_1=4$, and $t=2$, in Δl units, with $\Delta l=0.25\text{mm}$.

WR28 waveguide with a resonant square iris of dimensions $a_1=4\text{mm}$ and $b_1=1\text{mm}$, and width $t=0.5\text{mm}$ has been simulated with a node of equal sides $\Delta l=0.25\text{mm}$. The lengths of the problem in Δl units are $a=28$, $b=14$, $a_1=16$, $b_1=4$, and $t=2$. The amplitude of the S_{11} parameter for the system is plotted in Fig.6 for the standard TLM solution, the proposed TLM solution, and the TE_{m}^x mode matching results taken from [7]. The figure clearly indicates that the standard TLM mesh is able to predict the general behavior of the parameter, but provides an erroneous value of both the resonance frequency and the amplitude of S_{11} at this point. In contrast, the proposed nodes provide an accurate solution of the problem even near the resonant region.

4 CONCLUSIONS

In this paper, new modified TLM nodes with stubs have been proposed to model the existence of special conducting structures usually found in microwave systems. These nodes eliminate the problem existing in the standard formulation of the TLM method in which specially difficult points such as corners and bends are only indirectly modeled. The improvement provided by these nodes is present but not relevant if the problem is not critically dependent on frequency, but a significant improvement is demonstrated in resonant problems. Finally, it is interesting to note that the simultaneous use of standard and modified nodes provides a greater flexibility to the TLM method, since now conducting parts can be located at the center or between the nodes.

ACKNOWLEDGEMENT

This work was supported in part by 'Comisión Interministerial de Ciencia y Tecnología (CICYT)' of Spain under project number TIC95-0465. The authors would also like to thank Christine M. Laurin for her help in preparing the manuscript.

REFERENCES

- [1] A.P. Duffy, T.M. Benson, C.Christopoulos, and J.L. Herring, "New methods for accurate modeling of wires using TLM," *Electron. Lett.*, vol. 29, no. 2, pp. 224-226, Jan. 1993.
- [2] J.S. Nielsen and W.J.R. Hoefler, "Modification of the condensed 3-D TLM node to improve modeling of conductor edges," *IEEE Microwave Guided Wave Lett.*, vol. 2, no. 3, pp. 105-107, March 1992.
- [3] B. Bader and P. Ruser, "Modelling of edges and corners in the alternating transmission line matrix (ATLM) scheme," *Electron. Lett.*, vol. 32, no. 20, pp. 1897-1898, Sep. 1996.
- [4] Z. Chen, M.M. Ney, and W.J.R. Hoefler, "A new finite-difference time-domain formulation and its equivalence with the TLM symmetrical condensed node," *IEEE Trans. Microwave Theory Tech.*, vol. 39, no. 12, pp. 2160-2169, Dec. 1991.
- [5] P.B. Johns, "A symmetrical condensed node for the TLM method," *IEEE Trans. Microwave Theory Tech.*, vol. 35, no. 4, pp. 378-382, Apr. 1987.
- [6] H. Magán, J.A. Porti, O. Torres, and J.A. Morente, "Condiciones de contorno de banda ancha para el método TLM basadas en filtros FIR (Finite Impulse Response)," *XI Symposium Nacional de la URSI*, vol. 1, pp. 17-20, Madrid, Sept. 1996.
- [7] J. Bornemann and R. Vahldieck, "Characterization of a class of waveguide discontinuities using a modified TE_{m}^x mode approach," *IEEE Trans. Microwave Theory Tech.*, vol. 38, no. 12, pp. 1816-1822, Dec. 1990.